

A Design Scheme for Electromagnetic Shielding Clothes via Numerical Computation and Time Domain Measurements

Satoru KUROKAWA^{†a)} and Toru SATO^{††}, *Regular Members*

SUMMARY Electromagnetic shielding clothes for reducing human exposure to radio waves have been commercialized. However, their effect has so far been confirmed only in the form of the raw material. In this paper, we develop a new compact scheme for measuring electromagnetic radiations using a short dipole antenna and Gaussian pulses in order to evaluate the effect of the shielding clothes over a wide frequency range with the aid of time-domain measurements and FDTD computation. The proposed method is based on a time-domain analysis technique and pulse compression technique, which enables the user to separate the direct transmission wave from the reflection from the floor as well as from the refracted wave around the neck of the clothes. The direct advantage is that measurements can be made in an ordinary laboratory without the function of an electromagnetic anechoic chamber. Also, we can separate direct transmission wave and diffraction wave from the measurement result by using pulse compression technique, then each frequency characteristic of the shielding shirt can be evaluated. The performance of the separation is confirmed by comparing the measurements with those of a shirt with no opening. We further demonstrate the possibility of predicting the effective conductivity of the material as a function of frequency by comparing the measured results with realistic FDTD computations, which will enable us to design a shielding shirt via numerical means.

key words: *electromagnetic shielding clothes, time domain measurement, FDTD method, effective conductivity, numerical evaluation scheme*

1. Introduction

International standard has been set for human exposure to electromagnetic field emission and also for EMS regulations [1], [2]. We have developed special shielding clothes that reduce human exposure to radio waves radiated from 800 MHz mobile phones, and also the evaluation scheme for the clothes [3].

A few companies are developing shielding clothes which is made of metal plated fiber with high conductivity for reducing the human exposure to radio waves [4]. However, their effect has so far been confirmed only in the form of the raw material [5], [6], due to the lack of effective means for evaluating the shielding effect of the clothes in a realistic situation.

Here we develop a new compact scheme for measuring electromagnetic radiations using a short dipole antenna and Gaussian pulses in order to evaluate the effect of the shielding clothes over a wide frequency range. The pro-

posed method is based on a time-domain analysis technique and pulse compression technique [7], [8], which enables the user to separate the direct transmission wave from the reflection from the floor as well as from the refracted wave around the neck of the clothes. It is thus possible to evaluate the shape effect of clothes on the electromagnetic shielding performance in an ordinary laboratory.

After presenting the measurement scheme and the experimental setup, we explain the technique to decompose the received waves, which consists of the direct transmission wave and the refracted wave around the neck of the clothes, from other components such as reflections from the floor. Then we evaluate the shielding performance of the clothes, including the limitations on the evaluation of the diffraction wave from the neck of the clothes. Further, we compare the proposed time domain method with that by using a conventional network analyzer. Finally, we examine the experimental result by comparing with numerical results obtained with FDTD method by using a realistic phantom shape. The result suggests the possibility of predicting the conductivity of the material, which will enable us to design a shielding shirt via numerical means.

2. Measurement Scheme and the Experimental Setup

The proposed scheme is a time-domain method employing Gaussian impulses of about 2-nsec pulse width and a short dipole antenna whose length is 40 mm+40 mm. The experimental setup is schematically shown in Fig. 1. The transmitting antenna is set 1.3 m above the floor at 50 cm distance in front of the phantom body, which is a container of about 200 mm × 440 mm × 700 mm size filled with 0.4% NaCl water solution [9]. The receiving probe of 10 mm+10 mm length is set horizontally and vertically at three heights of 1.300 m, 1.325 m and 1.350 m, respectively, at a depth of 10 mm from the front side of the phantom. The receiving probe and its alignment are schematically shown in Fig. 2. The Gaussian pulses are generated with model 1000D of Picosecond Pulse Labs Inc. Time domain waveforms are measured with 54750A+54754A oscilloscope of Agilent Technology Inc. It synchronizes with the transmitted Gaussian pulses, and measured data are averaged for 4096 times.

The measurements are made for two different setups of the shielding clothes around the phantom; one is the phantom only, the other is the phantom covered by a round neck underwear which is made of silver plated fiber. The fabric form of the clothe used for the shirt is schematically shown

Manuscript received April 4, 2003.

Manuscript revised May 30, 2003.

[†]The author is with National Institute of Advanced Industrial Science and Technology, AIST Tsukuba Central 2, Tsukuba-shi, 305-8568 Japan.

^{††}The author is with the Graduate School of Informatics, Kyoto University, Kyoto-shi, 606-8501 Japan.

a) E-mail: satoru-kurokawa@aist.go.jp

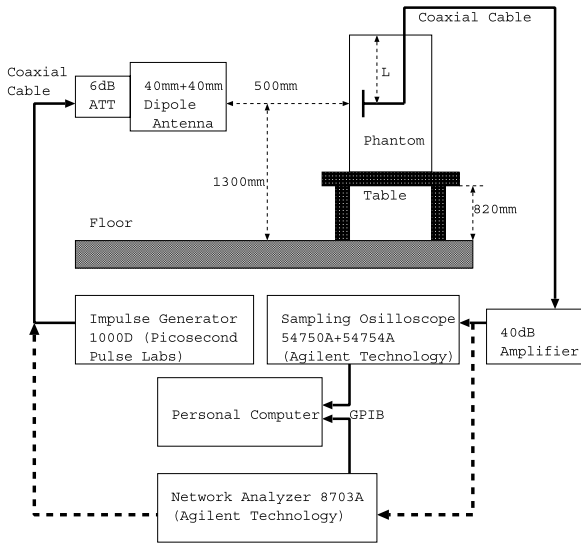


Fig. 1 Experimental setup.

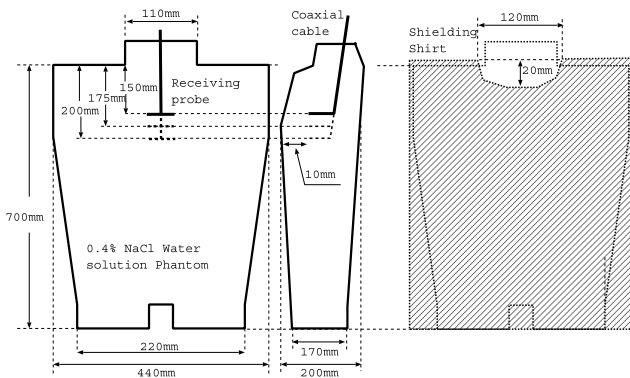


Fig. 2 Shape of the phantom and the location of the receiving probe.

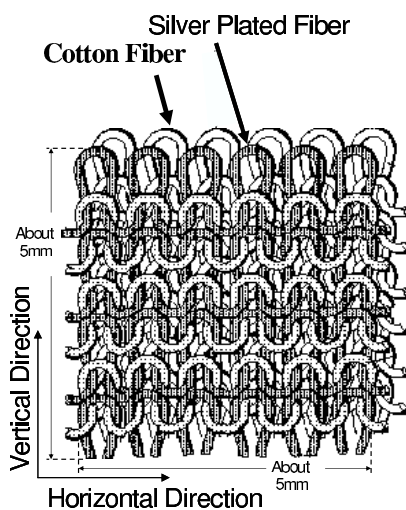


Fig. 3 The fabric form of the clothe used for the shirt.

in Fig. 3. The near-field shielding effect of the clothe used for the shirt is shown in Fig. 4 which is measured by using KEC method [10]. This result shows that the shielding effect

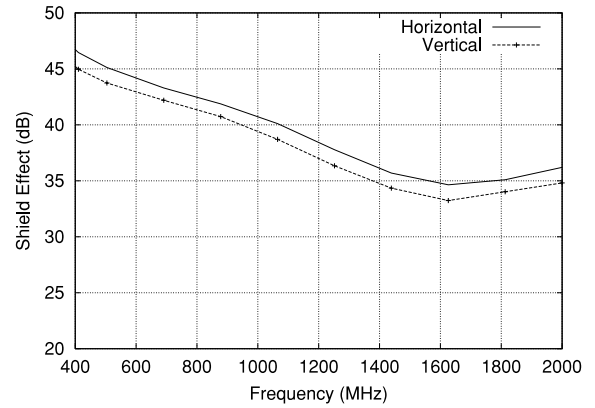


Fig. 4 Near-field shielding effect by KEC method.

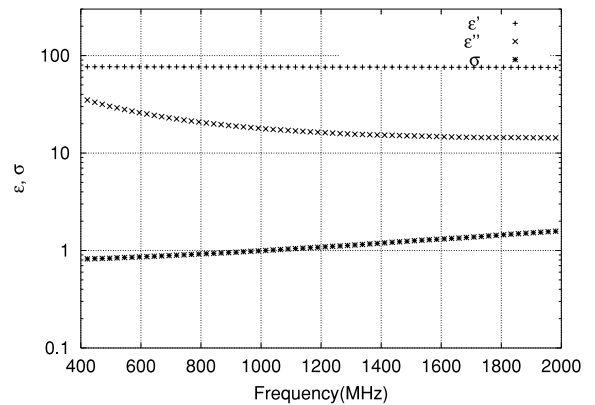


Fig. 5 Electrical property of 0.4% NaCl water solution phantom.

for the vertical polarization is about 1.0 dB to 1.5 dB lower than the horizontal one. Electrical property of 0.4% NaCl water solution phantom is shown in Fig. 5 which are measured with 8720B Network Analyzer and 85070D dielectric probe kit of the Agilent Technology Inc. ϵ'_r and ϵ''_r show the real part and the imaginary part of complex permittivity, respectively. σ shows the conductivity calculated by Eq. (2).

$$\epsilon_r = \epsilon'_r - j\epsilon''_r \quad (1)$$

$$\sigma = \omega\epsilon_0\epsilon''_r \quad (2)$$

3. Measurement Results

3.1 Time Domain Waveforms

Figures 6 and 7 show the received signal waveform and frequency characteristics for the case of the phantom without shielding clothes, respectively. After the direct wave is observed at about 6nsec delay, undesired reflected waves from the floor and the ceiling are observed around 9nsec and 11nsec. Figures 8 and 9 shows the received signals for the case of the round neck shirts at three receiving heights of horizontal and vertical antenna setup, respectively. $L = 200$ mm, $L = 175$ mm and $L = 150$ mm in Figs. 8 and 9 shows that measurement result of the distance of the antenna

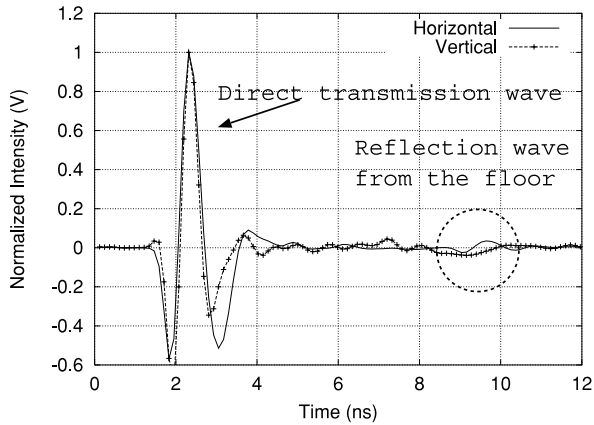


Fig. 6 Measured signal for the phantom only.

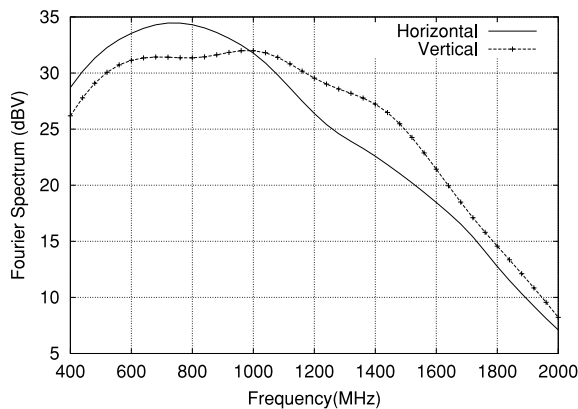


Fig. 7 Frequency characteristic for the phantom only.

from the floor is 1300 mm, 1325 mm and 1350 mm, respectively. [No Diffract] in Figs. 8 and 9 indicates measurement results of the shielding shirt that has minimum neck size of about 5 mm, with which the diffraction wave from the neck can be neglected. It can be thus regarded as a reference to show the effect of the direct transmitted wave.

For the horizontal antenna setup, the peak value of the diffraction wave from the neck at 7–8 ns does not increase appreciably as L decreases, and it is less than 0.3 times the peak value of the direct wave even for the case of $L = 150$ mm. On the other hand, the level of the diffracted wave remarkably increases as L decreases for the vertical antenna setup, which amounts to about 5 times the peak level of the direct wave for $L = 150$ mm. These results clearly show the dependence of the magnitude of diffraction on the antenna polarization setup. The magnitude of the direct transmission wave is about the same for both antenna setups.

3.2 Separation of Wave Components Using Pulse Compression Technique

It will be effective in designing a shielding shirt if we can separate the transmitted waves through the material from the diffracted waves around the neck. It is, however, difficult to

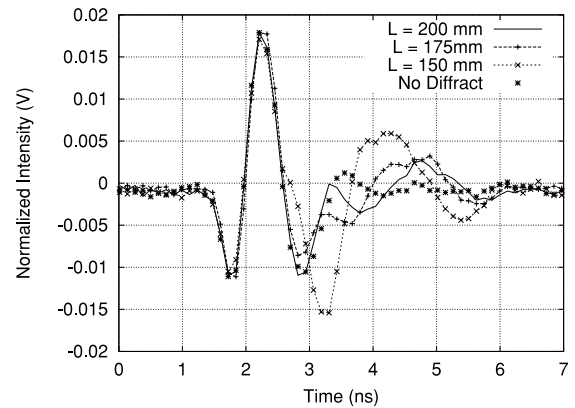


Fig. 8 Measured signal for the shirt with horizontal antenna setup.

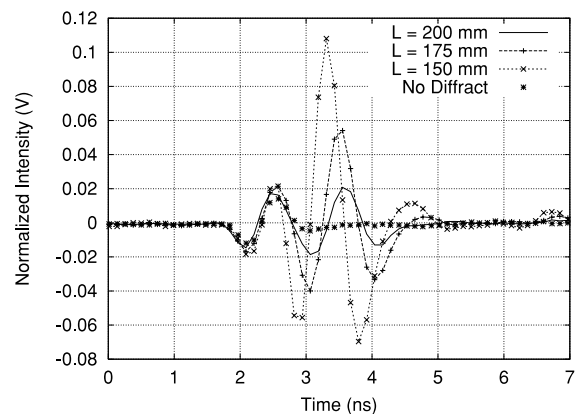


Fig. 9 Measured signal for the shirt with vertical antenna setup.

separate these two components directly from the measurements presented in the previous section. Here we examine a time domain method to separate these components, which is based on the pulse compression technique using the Wiener filter [7], [8].

The Wiener filter $w_{ph}(\omega)$ is expressed in the frequency domain in terms of the Fourier transform of the measured signal $E_{ph}(\omega)$ in the absence of the clothes as

$$w_{ph}(\omega) = \frac{E_{ph}^*(\omega)}{\eta |E_{ph}(\omega)|^2 + (1 - \eta)}, \quad (3)$$

where η is the parameter determined from the signal-to-noise ratio, and controls the filter response between the matched filter and the inverse filter. The compressed waveform in the frequency and the time domains are obtained by

$$I_{sh}(\omega) = E_{sh}(\omega) \cdot w_{ph}(\omega) \quad (4)$$

and

$$i_{sh}(t) = \mathcal{F}^{-1}(I_{sh}(\omega)), \quad (5)$$

respectively, where $E_{sh}(\omega)$ is the measured signal with the shielding clothes, and \mathcal{F}^{-1} denotes the inverse Fourier transform.

Figure 10 shows the variation of the compressed waveform with η of the Wiener filter by using the measured signal

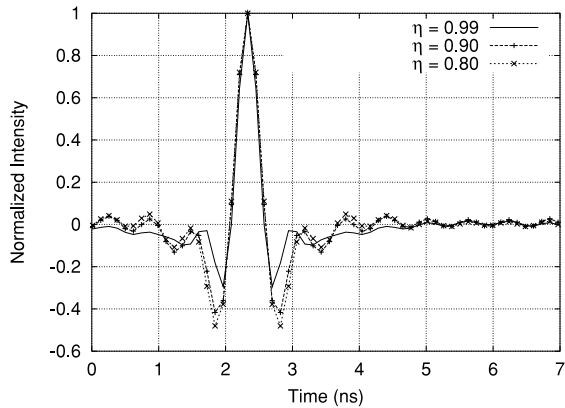


Fig. 10 Compressed pulse waveform with various η for the vertical antenna setup.

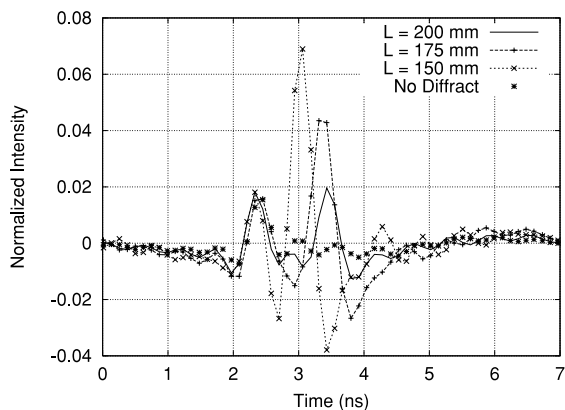


Fig. 11 Compressed pulse waveform for the vertical antenna setup.

in case of the phantom only.

Figure 11 shows the compressed pulse waveforms for the vertical antenna setup. Comparing this figure with Fig. 9, it is found that the peaks are better separated because the undershoot components are suppressed by the pulse compression. Almost complete separation can be obtained for $L = 200$ mm, for which the two components are examined individually below.

In order to separate the direct and the diffracted waves, we apply two Hanning-type (raised cosine) time windows $H_{\text{dir}}(t)$ and $H_{\text{dif}}(t)$ with an overlap region of 2.8–3.0 ns, which seems to be the boundary between the two components. Then we reconstruct the original time series of the both components by applying the inverse Wiener filter in the frequency domain as given by

$$E_{\text{shdir}}(\omega) = w_{\text{ph}}^{-1}(\omega) \cdot \mathcal{F}\{i_{\text{sh}}(t) \cdot H_{\text{dir}}(t)\} \quad (6)$$

$$E_{\text{shdif}}(\omega) = w_{\text{ph}}^{-1}(\omega) \cdot \mathcal{F}\{i_{\text{sh}}(t) \cdot H_{\text{dif}}(t)\} \quad (7)$$

Figure 12 shows frequency characteristics of the shielding effect for the direct and the diffracted components for $L = 200$ mm. Figure 13 is same as Fig. 12, but for the vertical antenna setup. The shielding performance of the shirt for the horizontal and vertical polarizations are computed by $S_{\text{H}}(\omega)$ and $S_{\text{V}}(\omega)$, respectively, defined by the fol-

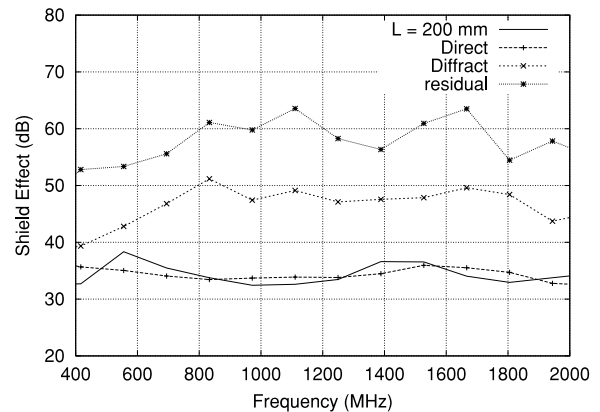


Fig. 12 Frequency characteristics of the direct transmission wave and the diffraction wave from the neck for the horizontal antenna setup.

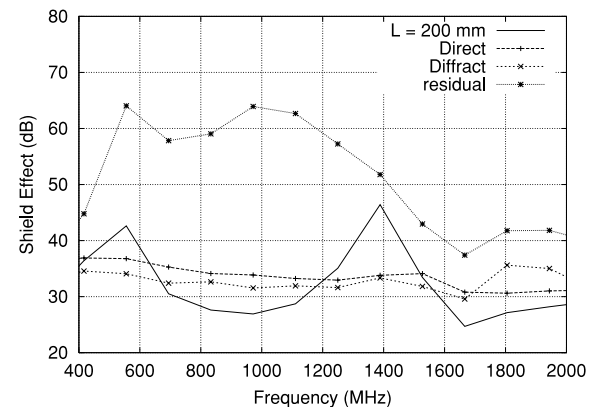


Fig. 13 Frequency characteristics of the direct transmission wave and the diffraction wave from the neck for the vertical antenna setup.

lowing equations.

$$S_{\text{H}}(\omega) = |E_{\text{hph}}(\omega)|^2 / |E_{\text{hph}}(\omega) - E_{\text{hsh}}(\omega)|^2 \quad (8)$$

$$S_{\text{V}}(\omega) = |E_{\text{vph}}(\omega)|^2 / |E_{\text{vph}}(\omega) - E_{\text{vsh}}(\omega)|^2, \quad (9)$$

where subscript [ph] denotes the electric field for the case of phantom only, and [sh] for the shielding shirt.

Curves indicated as [Direct] and [Diffract] in the figure show the direct and diffracted wave components, respectively, separated from the measured signal by the proposed method. Open square symbols corresponding to [No-Diffract] show the case of the minimum neck size used as a reference. The very good agreement of [Direct] and [No-Diffract] data of less than 1 dB for most of the frequency range clearly verifies the performance of the proposed separation scheme. The curve indicated as [Residual] shows the shielding performance corresponding to the level of the residual component of the [No-Diffract] data after rejection of the direct wave, which shows the evaluation limit of the proposed procedure.

From these figures it is clear that the shielding performance of the shirt for the direct transmission wave is roughly constant in the range of 30–36 dB for both horizontal and vertical polarizations throughout a wide frequency

range of 400–2000 MHz. The major difference in the total shielding performance with polarizations comes from the magnitude of the diffracted component. While it is always higher than 40 dB for the horizontal polarization, it is around 35 dB for the vertical component. The large variation of the total performance with frequency for the vertical polarization is apparently due to interferences between the direct and diffracted components of comparable magnitude.

The reason of higher level of the diffracted component for the vertical polarization is probably due to the fact that the opening of the neck is mainly in the horizontal plane, where the vertical electric field is dominant. A further analysis of the electric field distribution is needed for detailed examination.

The result shown here clearly demonstrates the capability of the proposed time domain method in evaluating and designing shielding shirts based on the shielding performance of the material itself in the form of the shirt as well as the effect of diffracted waves around the opening of the shirt over a wide frequency range.

3.3 Time Domain Waveforms by Using Network Analyzer

An alternative means of time domain evaluation of the shielding shirt may be that using the time domain function of a network analyzer. For comparison with the proposed method presented in this paper, we make a similar measurement as that in the previous section with a setup shown in Fig. 1 for the case of the phantom only.

Time domain waveforms are measured with 8703A network analyzer of Agilent Technology Inc. using its built-in time domain function. Measurement is carried out after a 2-port calibration at the end of the coaxial cable. Although a calibration might be made with the transmitting antenna and the receiving probe inserted in the phantom are connected to the cable, it turned out to be not realistic because reflections from the floor contaminates the calibration.

Figure 14 shows the received waveform for the phantom only. Measurement result for the both antenna setups clearly shows that the generated pulse width of more than

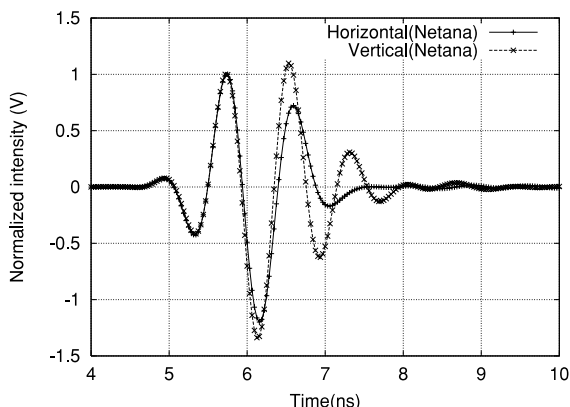


Fig. 14 Measured signal for the phantom only by using network analyzer.

3 ns prohibits us to separate the direct and the diffracted wave components. This is apparently due to the window shape, which is designed to fulfill requirements for a sharp cutoff in the frequency domain, employed for the network analyzer. This result clearly shows the advantage of our proposed scheme for shielding performance measurements of the shirt to the time domain function of conventional network analyzers.

4. Evaluation of the Shielding Performance with Numerical Computations

4.1 Calculation Conditions

In order to examine the shape effect of the shirts further, we made numerical computations using FDTD method [11]. We divide the calculation space of 900 mm × 850 mm × 600 mm into 360 × 340 × 240 cells with the grid size of 2.5 mm and the time step of 4.8 psec. The computational setup is shown in Fig. 15. The Liao absorption boundary condition is used [12]. Although PML absorption boundary condition is considered to give the best performance, we employed the Liao condition because it is found to give almost identical result as PML for the current case, and the former is appreciably faster and is more memory efficient.

The relative dielectric constant and the conductivity of the phantom is set to 77.4 and 1.1, respectively, based on the measurement result over the frequency range of 400–2000 MHz. It should be noted that values above about 1400 MHz may contain larger numerical errors as the grid size is more than 1/10 of the wavelength at these frequencies. The clothes are separated by 5 mm (2 cells) from the phantom surface. Shape of the clothes used for computation is shown in Fig. 2. Figure 16 shows the computed wave-

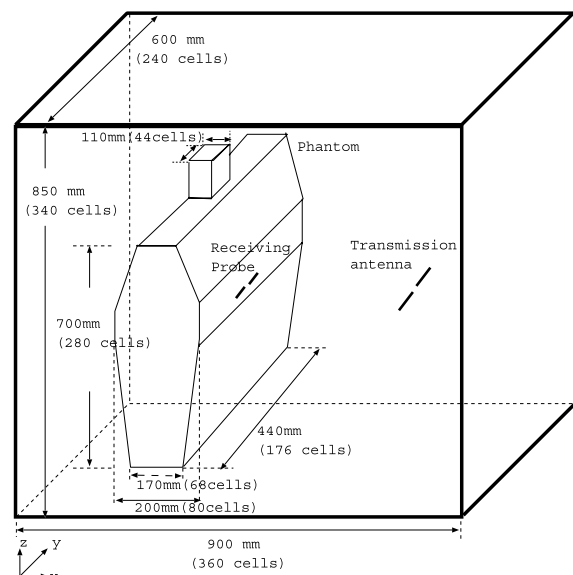


Fig. 15 Setup for the FDTD calculation space.

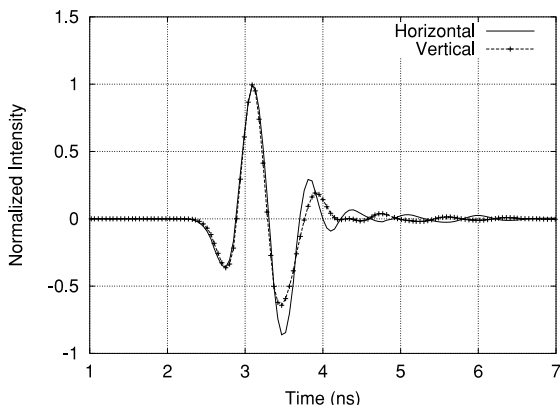


Fig. 16 Computed signal for the phantom only.

forms at the receiving probe for the horizontal and the vertical antenna setups. The computed waveform is slightly shorter than that in Fig. 6, reflecting the fact that the antenna bandwidth is narrower in the actual measurement than in the computation.

4.2 Effect of Conductivity

In this section, we examine the effect of conductivity of the material on transmitted waves. In almost all cases, shielding clothes are made by metal plated fiber. Unlike metallic films, it is not easy to measure the conductivity of the cloth knitted with metal plated fiber. Performance of shielding clothes has thus been evaluated by the conductivity of the material used for plating, or that of the cloth by the KEC method [10].

We estimate the effective conductivity of the clothes, which is defined as the conductivity of uniform material which gives the same shielding performance as the clothes under examination, using the FDTD method. In order to compare the shielding performance, conductivity of the material is set to $\sigma = 100 \text{ S/m}$, 200 S/m , 300 S/m , 400 S/m and $1.0 \times 10^6 \text{ S/m}$. The position of the receiving antenna is set to $L = 200 \text{ mm}$, which case showed the best performance in terms of the effect of diffraction waves by experimental results.

Figures 17 and 18 show computed signal waveforms for various conductivity of the shirt for the horizontal antenna setup and vertical antenna setup, respectively. For both antenna polarization setups, The relative magnitude of the transmission component decreases as the conductivity is increased, to the extreme case of $\sigma = 1.0 \times 10^6 \text{ S/m}$ where only the diffraction wave is observed.

Figure 19 shows the corresponding frequency characteristics of the shielding performance for the horizontal antenna setup after separation of the direct and the diffraction waves from the calculation result by using the same pulse compression technique as described in the previous section with $\eta=0.99$, except for the case of $\sigma = 1.0 \times 10^6 \text{ S/m}$, which is considered to consist entirely of the diffracted wave. Lines denoted as ‘Exp [Direct]’ and ‘Exp [Diffract]’

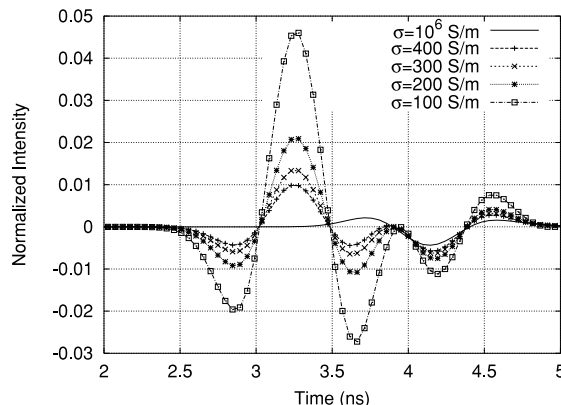


Fig. 17 Computed signal waveform of the shielding shirt with various conductivity for the horizontal antenna setup.

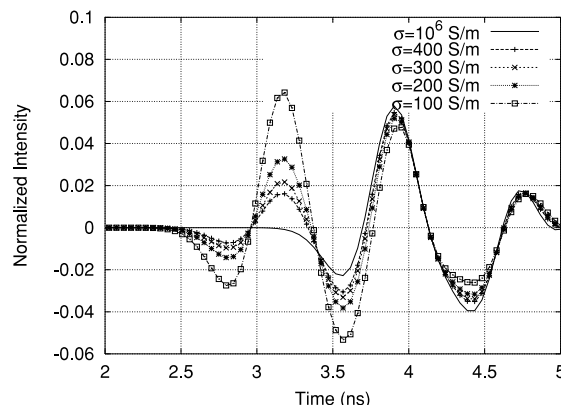


Fig. 18 Computed signal waveform of the shielding shirt with various conductivity for the vertical antenna setup.

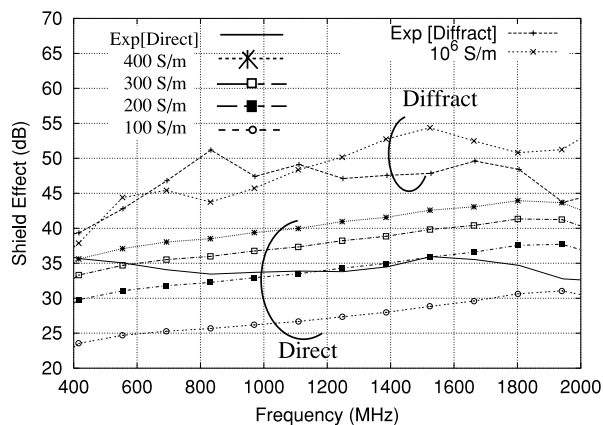


Fig. 19 Comparison of the measured and computed shielding effect of the shielding shirt for the horizontal antenna setup.

show direct wave and diffraction wave of the shielding shirt by using pulse compression technique copied from Fig. 12 The measured curves closely follow the computed ones. Calculation result for the case of $\sigma = 1.0 \times 10^6 \text{ S/m}$ shows the shielding performance for the diffraction wave from the neck, and other cases show the shielding effect against the

direct transmission wave.

First, we compare the frequency characteristics of the FDTD calculation results with those of the measured results. The shielding effect of the measured data for the horizontal antenna setup (solid line in Fig. 19) agrees with that of the computed result of 200 S/m for the frequency range of 1000–1600 MHz, and of 100–200 S/m for the frequency range of 1600–2000 Hz. Here we refer to the best match computed conductivity as the ‘effective conductivity.’ For a lower frequency range, it seems to decrease from about 400 S/m to 200 S/m as the frequency increases. The decrease of this effective conductivity in increasing frequency can be explained that the relative interval of the weaving pattern in terms of the radio wavelength increases with frequency, and thus the transmission through the material increases.

Next we compare the shielding performance for the diffraction wave. Measured diffraction wave component (dotted line with + symbol) agrees well with the computed result for high conductivity ($\sigma = 10 \times 10^6$ S/m) case within the error of about 5 dB. Considering the fact that a high value in this figure means a very weak received signal, difference of the computational and experimental setups may explain the disagreements. They seem to be due partly to the difference in the actual and computed shape of the shirt, especially to the rectangular opening of the neck shape in the computation while the actual neck has an elliptical opening, and partly to the separation procedure of the direct and the diffracted waves from the measured data. Further improvements of computational method as well as the data processing will be required for better agreement.

As is demonstrated here, the proposed scheme provides a direct means of estimating the effective conductivity of a shielding shirt in a realistic condition. It is thus possible to design a variety of shirt with desired performance and shape based on numerical evaluations by using FDTD method.

5. Conclusion

We developed a compact and wideband evaluation scheme for electromagnetic shielding clothes by making time-domain measurement using short dipole antennas, Gaussian impulse and pulse compression technique. The shielding effect can be measured over the range of 400 MHz to 2 GHz from single experiment. This method enables separation of multiple components such as the direct transmission wave and diffracted waves, as well as reflections from the floor and the ceiling. The direct advantage is that measurements can be made in an ordinary laboratory without the function of an electromagnetic anechoic chamber and separation of the direct transmission wave and diffracted waves by using pulse compression technique. The performance of the separation scheme was examined by comparing the results with that for a shirt with no opening at the neck, which is used as a reference showing the effect of the direct transmission component only. The very good agreement of less than 1 dB for most of the frequency range confirms the effectiveness

of the proposed scheme.

We further made best use of this feature of decomposition in evaluating the neck design of the shielding shirts. It is found that the diffraction wave is dominant for the vertical antenna setup, and the interference between the transmission wave and the diffraction wave determines the shielding performance. Effect of the conductivity is evaluated for the round-neck shirt by comparing the measured frequency characteristics with that computed for uniform materials with a variety of conductivity by using FDTD method. It was found that the shirt has an effective conductivity of 100–400 S/m for 400 MHz to 2 GHz.

The proposed scheme will enable us to predict the shielding performance of a shirt with arbitrary design numerically by using FDTD method. We plan to apply the developed method to evaluate the performance of various types of shielding clothes such as Y shirts and jackets.

Acknowledgment

We would like to thank Gunze Inc. and Goldwin Inc. for their help in developing the measurement scheme as well as for providing the material.

References

- [1] IEC 60601-1-2, Medical electrical equipment Part 1: General requirements for safety 2. Collateral Standard: Electromagnetic compatibility—Requirements and tests, p.17, 1993.
- [2] Evaluating Compliance with FCC Guidelines for Human Exposure to Radio frequency Electromagnetic Fields. Additional Information for Evaluating Compliance of Mobile and Portable Devices with FCC Limits for Human Exposure to Radio frequency Emissions, SUPPLEMENT C Edition 97-01 to OET BULLETIN 65 Edition 97-01, p.79, Dec. 1997.
- [3] S. Kurokawa and T. Sato, “A compact time-domain evaluation scheme for electromagnetic shielding clothes,” KJJC-AP/EMC/EMT 2001, pp.86–89, Sept. 2001.
- [4] Goldwin Corporation, “Electromagnetic Shielding Blouses for the pilot,” <http://1for1.co.jp/index.html> (in Japanese).
- [5] Japan Chemical Fibers Association, “The guideline of the evaluation method of an electromagnetic wave shield material,” http://www.fcc.co.jp/JCFA/f6_soza.html (in Japanese).
- [6] I. Wu and O. Hashimoto, “An electric shielding effect of near field for perfect conducting shield arranged in front of oval human model,” IEICE Trans. Commun. (Japanese Edition), vol.J84-B, no.1, pp.150–152, Jan 2001.
- [7] S. Kurokawa and T. Sato, “Experimental study of estimating free space radiated emission by using FDTD analysis and time domain measurement,” IEICE Technical Report, EMCJ2000-24, 2000.
- [8] S. Kurokawa and T. Sato, “Experimental study of estimating indoor propagation by using small dipole antennas,” Technical Report of IEEJ, EMT-00-74, 2000.
- [9] K. Ito, S. Kurokawa, and K. Ueno, “Interstitial applicators using thin cable for hyperthermia,” IEICE Technical Report, AP88-75, 1988.
- [10] Kansai Electronic Industry Development Center, “Introduction of KEC measurement method,” <http://www.kec.or.jp/menu2/6.htm> (in Japanese).
- [11] K.S. Kunts and R.J. Lubbers, The finite Difference Time Domain Method for Electro-Magnetics, p.448, CRC Press, Boca Raton, USA, 1993.
- [12] Remcom Inc., “User’s Manual for XFDTD the Finite Difference

Time Domain Graphical User Interface for Electromagnetic Calculations," Version 5.0, p.133, 1998.



Satoru Kurokawa received his B.E., M.E. degrees in electrical engineering from Chiba University, Chiba, Japan in 1987, and 1989, and entered Department of Communication and Computer Engineering, Graduate School of Informatics, Kyoto University in 1999. He has been at Kyoto Prefecture since 1989. From 1994 to march 2003, he was a staff of Research and Development Division, Kyoto Prefectural Comprehensive Center. He has been at National Institute of Advanced Industrial Science and Technology since April 2003 and is currently a staff of Electromagnetic Waves

Division. His research interest has been EMI Measurement and Small Antenna. He is a member of the Institute of Electrical and Electronics Engineers.



Toru Sato received his B.E., M.E., and Ph.D. degrees in electrical engineering from Kyoto University, Kyoto, Japan in 1976, 1978, and 1982, respectively. He has been at Kyoto University since 1983 and is currently a Professor of Department of Communications and Computer Engineering, Graduate School of Informatics. His major research interests have been system design and signal processing of atmospheric radars, radar remote sensing of the atmosphere, observations of precipitation using

radar and satellite signals, radar observation of space debris, and signal processing for subsurface radars. He was awarded Tanakadate Prize in 1986. He is a member of the Society of Geomagnetism and Earth, Planetary and Space Sciences, the Japan Society for Aeronautical and Space Sciences, the Institute of Electrical and Electronics Engineers, and American Meteorological Society.